# Time-domain analysis of optical comb offset frequency variations: phase-only line-by-line shaping approach

**José Caraquitena,[1,2,*] Zhi Jiang,[1,3] Daniel E. Leaird,[1] and Andrew M. Weiner[1]**

[1]*School of Electrical and Computer Engineering, Purdue University, 465 Northwestern Avenue, West Lafayette, Indiana 47907-2035, USA*

[2]*Current address: Nanophotonics Technology Center, Universidad Politécnica de Valencia, Camino de Vera s/n, Valencia 46022, Spain*

[3]*Current address: Biophotonics Imaging Laboratory, Beckman Institute for Advanced Science and Technology, University of Illinois at Urbana-Champaign, Urbana, Illinois 61801, USA*

**Corresponding author: jcaraqui@ntc.upv.es*

Received July 25, 2008; revised October 17, 2008; accepted October 20, 2008; posted October 21, 2008 (Doc. ID 99416); published December 16, 2008

We investigate the effect of shifting an optical frequency comb on the resultant time-domain waveform generated via phase-only line-by-line pulse shaping. By considering a particular spectral line-by-line filter, comb shifts, i.e., offset frequency variations, are evaluated in a simple way from the changes in the temporal intensity waveform. Theoretical predictions are confirmed by experimental results. As a practical application, we estimate the magnitude of comb offset frequency fluctuations of a harmonically mode-locked fiber laser from noise in the waveforms measured with a sampling scope. © 2008 Optical Society of America

*OCIS codes:* 320.5540, 140.4050, 120.3930, 070.6760.

## 1. INTRODUCTION

Optical pulse shaping is a widely adopted technique in which intensity and phase manipulation of optical spectral components allow synthesis of user-specified ultrashort pulse fields according to a Fourier transform relationship [1]. Traditionally pulse shapers have addressed spectral lines in groups at low spectral resolutions. This results in shaped waveform bursts that are separated in time with low duty factors. On the other hand, over the past decade, considerable interest has arisen in optical frequency combs, i.e., spectra consisting of an evenly spaced series of discrete and mutually coherent spectral lines with frequency spacing equal to the pulse repetition rate $f_{rep}$ [2]. Self-referencing techniques have allowed stabilization of the full set of optical frequencies across octave-spanning mode-locked laser comb spectra [2], contributing to dramatic improvements in the precision of optical frequency metrology and synthesis [3,4]. Such self-referenced and stabilized mode-locked combs generally operate at repetition rates of ~1 GHz and below. Frequency combs at higher repetition rates (e.g., 10 GHz) are also of interest for applications, such as telecommunications, although available high rate comb sources typically lack the optical frequency stability of the lower rate mode-locked frequency combs. Combining pulse shaping with optical frequency comb sources is likely to lead to new capabilities not previously available. Here, in order to approach true optical arbitrary waveform generation, the phase and amplitude of each individual comb line should be independently controlled on a line-by-line basis [5–9]. A high resolution pulse shaper capable of implementing line-by-line control can generate shaped waveforms spanning the full time period ($T=1/f_{rep}$) between input pulses (100% duty factor). Therefore, in the line-by-line regime, waveform contributions arising from adjacent pulses in the input train overlap in time and interfere. The effect of the interference depends on the relative phase between adjacent input pulses, which is proportional to the comb offset frequency. Consequently, time-varying shifts of the frequency comb translate into time dependent waveform noise in line-by-line pulse shaping. This coupling between comb frequency shifts and time-domain waveform changes is a fundamentally new aspect of line-by-line shaping that is not present in previous work on group-of-lines pulse shaping.

Due to limits in the spectral resolution of grating-based pulse shapers, line-by-line pulse shaping has been reported only at repetition rates of 5 GHz [6] and above. The first observation of waveform noise induced in line-by-line pulse shaping due to optical frequency fluctuations was reported in [10] by selecting two comb lines from a harmonically mode-locked fiber laser without active frequency stabilization. A selection of only two spectral lines from the broader input spectrum yields a cosine waveform in the time-domain. The experiments showed that waveform noise related to optical frequency fluctuations was much larger when the relative phase between the selected spectral lines was $\Phi=\pi$ compared with the case of $\Phi=0$. This difference was understood by observing that the largest waveform noise is expected at temporal positions where adjacent input pulses provide equal contributions and hence largest interference, which occurs exactly between the original pulses (at $T/2$). This time-domain picture provides a successful qualitative explana-

 

tion of the experimental results. A first quantitative investigation of the impact of optical frequency offsets on time-domain intensity waveforms generated via grating-based line-by-line pulse shaping was reported in [11]. More specifically, the influence of static offset frequency fluctuations on generated waveforms was analyzed for several simple passband filter functions (spectral amplitude filters) accompanied, in some cases, with spectral phase control. Only a few spectral lines of the frequency comb were involved in the filtering process. In the experiments reported in [11], the optical comb was generated by an electro-optic phase-modulated cw laser and the effects of static comb offsets were emulated by shifting the center wavelength of the cw laser.

In this paper, we evaluate the effect of time-varying comb offset frequency variations on phase-only line-by-line pulse shaping of a harmonically mode-locked fiber laser with repetition rate $f_{\mathrm{rep}}$, which we adjusted to either 9 or 10 GHz in these experiments. In contrast to earlier experiments from our group, here we retain all of the (~30) comb lines generated by the mode-locked laser. This provides better power efficiency and constitutes an example of pulse shaping with considerably more spectral control elements. We demonstrate, through simulations and experimental results, that the resultant time-domain waveforms change in a simple fashion with the optical comb shift and, as a result, comb offsets can be simply derived from these measurements. We then demonstrate that noise in the measured time-domain waveforms provides direct quantitative information about offset frequency fluctuations of the mode-locked laser comb.

The remainder of this paper is structured as follows. In Section 2, we introduce the specific spectral line-by-line filter considered throughout this paper. First, the effective spectral-filter response is numerically derived and the time-domain waveform variation as a function of the offset frequency is analyzed. Next, we describe the pulse-shaper setup and experimental results are reported. In Section 3, we estimate the offset frequency fluctuations of a harmonically mode-locked fiber laser by examining the noise found in the generated waveforms after line-by-line shaping. In Section 4, we conclude.

## 2. TWO-VALUED PHASE-ONLY LINE-BY-LINE SHAPING

### A. Theory

For a free-space grating-based pulse shaper, the effective frequency-domain transfer function $H(\omega)$ that characterizes its response as a linear filter can be obtained by convolving the programmable spatial masking function $M(x)$, defined by the liquid crystal modulator (LCM), with the Gaussian intensity profile of a single optical frequency beam

$$H(\omega)=\left(\frac{2}{\pi w_o^2}\right)^{1/2}\int M(x)e^{-2(x-\alpha\omega)^2/w_o^2}\mathrm{d}x, \qquad (1)$$

where $w_o$ is the Gaussian beam radius (half width at $1/e^2$ of intensity) and $\alpha$ is the spatial dispersion with units cm $(\mathrm{rad/s})^{-1}$ [1]. We consider a particular filter derived from a phase-only mask consisting of a two-valued periodic sequence $\{0,\Phi,0,\Phi,\ldots\}$ with $\Phi=\pi/2$, so that the same phase-shift is applied to every other line over the whole optical frequency comb. In the limit $w_o\to 0$, the pulse shaper provides perfect spectral resolution and the resultant spectral phase filter function is a scaled version of the spatial masking function [1] as shown in Fig. 1(a) (dashed curve). In practice, numerical simulations considering the finite spectral resolution of our shaper, according to Eq. (1), show that the effective phase filter is a smooth function (solid curve). On the other hand, the applied phase pattern induces a periodic frequency-dependent intensity transfer function as shown in Fig. 1(b). In the simulation, a linear spatial dispersion $\alpha=3.54e-13$ cm$(\mathrm{rad/s})^{-1}$ is considered, which coincides with that in our specific pulse-shaper design. Concerning the spatial mask, our LCM has a 100 $\mu$m pixel width and a corresponding frequency span of 4.5 GHz according to the value of $\alpha$; therefore each spectral line is controlled by every two pixels when the spectral line spacing is $f_{\mathrm{rep}}=9$ GHz. In addition, we assumed a beam width of $w_o=80$ $\mu$m. We arbitrarily choose zero relative offset frequency when the optical comb is centered on the frequency filter as shown in Fig. 1 (gray solid comb). The location of each spectral line is given by $f_n=f_o+nf_{\mathrm{rep}}$, where $f_o$ is the carrier frequency and $n$ is an integer.

In Fig. 2, we show the phase transfer function together with the comb for different offsets, namely, 0%, 25%, 50%, and 75%. Note that when the comb is shifted (gray combs), the effective phase-shifts applied to the spectral lines change in such a way that the phase-difference between adjacent lines is gradually decreased ultimately to a zero phase-difference for 50% offset frequency. By further increasing the offset, the phase-difference increases,

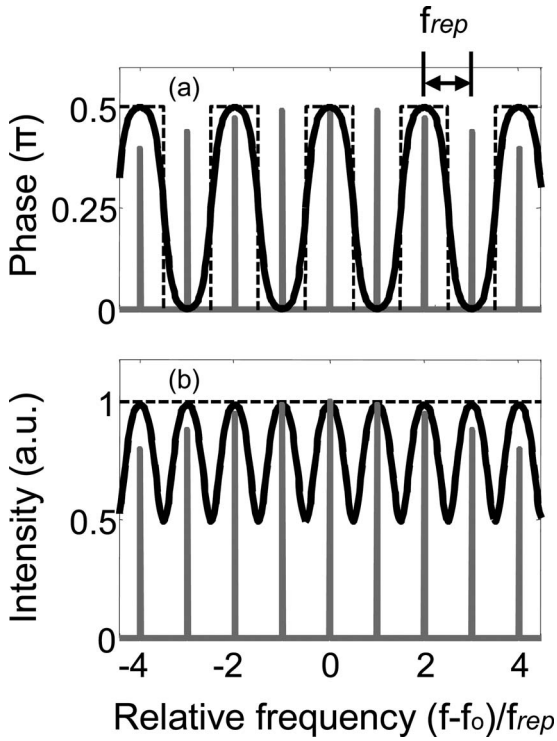


Fig. 1. (a) Phase and (b) intensity filter functions (solid curve) together with the optical comb for zero relative offset frequency. The mask function is also represented (dashed curve).

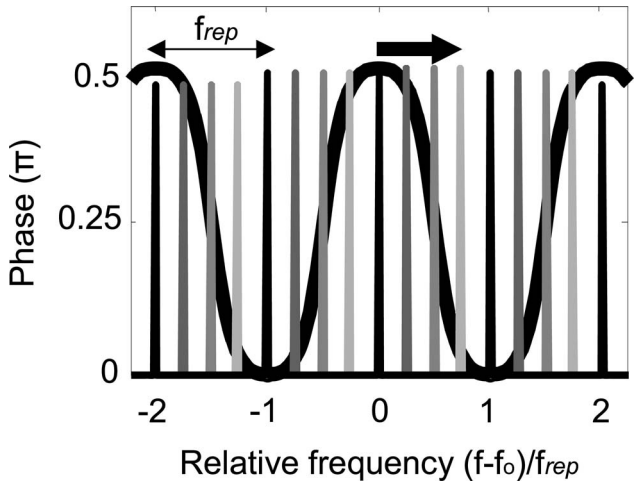


Fig. 2. Phase filter function (thick solid curve) and optical comb for different offsets. The effective phase-shifts imposed on the spectral lines of the comb change with the offset frequency. The horizontal arrow indicates the direction of detuning.

in absolute value, until approaching $\pi/2$ for 100% offset. This behavior is periodically repeated for larger offsets. In time-domain, for 0% offset the resultant intensity waveform is, according to the temporal Talbot effect [12,13], a doubled repetition-rate replica of the input pulse train. It is simple to demonstrate that two-times repetition-rate multiplication is still obtained for any other offset; however, adjacent pulses in each period have different peak-power values depending on the particular comb shift. In Fig. 3(a), we show the input pulse train considered in our numerical simulations, and Figs. 3(b)–3(e) show the output pulse trains for 0%, 25%, 50%, and 75% offset, respectively. A pulse width of 3 ps has been considered in the simulations. For 0% offset, a uniform two-times multiplied version of the input pulse train is obtained, as mentioned. When the comb is shifted, the peak-power at $T/2$ gradually decreases [see Fig. 3(c)], until dropping to zero just for 50% offset as shown in Fig. 3(d). If the comb is further shifted, the peak-power gradually increases [Fig. 3(e)]. Note that the intensity transfer function, shown in Fig. 1(b), behaves like a variable attenuator on the output waveform when the comb is shifted, without any influence on the time-domain waveform profile.

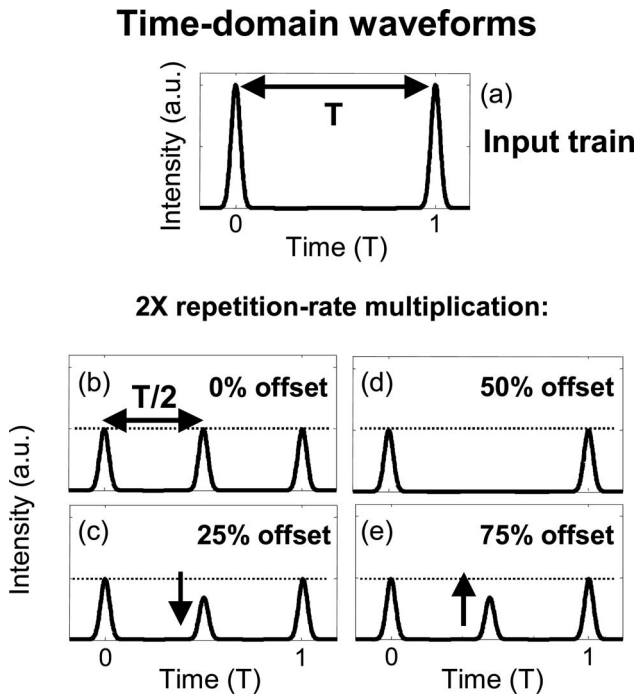


Fig. 3. Simulated time-domain waveforms. (a) Input pulse train. (b)–(e) Output trains with doubled repetition rate. The intensity-modulation in the output train depends on the frequency offset. For 50% offset, the pulse at $T/2$ is missing. The vertical arrows indicate intensity peak variations as the optical offset frequency increases.

We emphasize that the only effect of shifting the comb is a change in the ratio between $I(T/2)$ and $I(0)$ in the output multiplied train. This suggests the ratio $\Delta = I(T/2)/I(0)$ as a suitable parameter to evaluate the variations of comb offset. In Fig. 4, we show the calculated value of $\Delta$ as a function of the offset frequency. This interesting result shows that line-by-line shaping can transform comb shifts, in frequency-domain, into intensity-modulation, in time-domain.

### B. Experimental Setup and Results

A home-built actively mode-locked Er-fiber laser producing ~3 ps (full width at half maximum) pulses at a 9–10 GHz tunable repetition rate with a center wavelength of 1542.5 nm is utilized as the pulse source for our experiments. Spectral line-by-line control is performed by using a carefully designed pulse shaper [5], which includes an LCM array that allows us to independently manipulate both the amplitude and phase of individual spectral lines making up the mode-locked laser frequency comb. The resulting optical signal is characterized by using an optical spectrum analyzer (OSA) and a 20 GHz bandwidth photodiode followed by a sampling scope. In the experiment, we program the LCM to obtain a phase mask consisting of a periodic two-phase sequence $\{0, \pi/2, 0, \pi/2, \ldots\}$, according to the theory introduced in

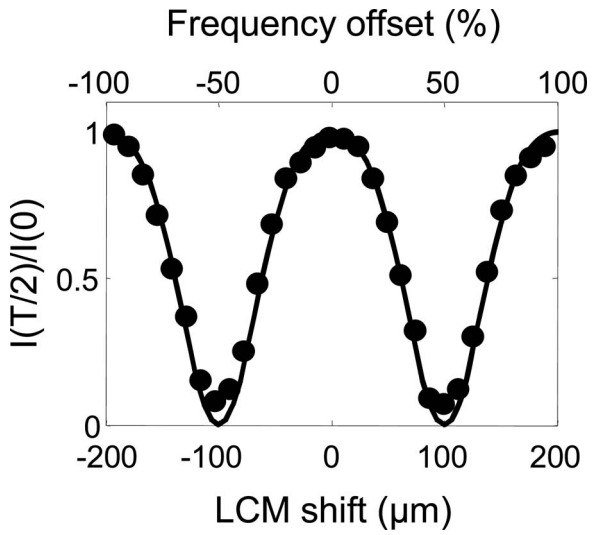


Fig. 4. Pulse-train modulation (solid curve) as a function of the offset frequency, calculated from the output pulse trains as those shown in Fig. 3. Measured (closed circles) intensity-modulation values are also represented.

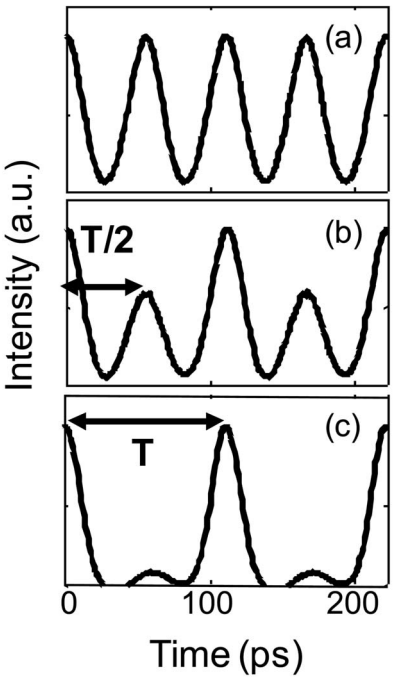


Fig. 5. Averaged sampling scope traces for (a) 0%, (b) 25%, and (c) 50% offset frequency, respectively.

Subsection 2.A, so that the same phase-shift is applied to every other line over the whole optical frequency comb.

To emulate the effect of comb offset frequency variation we instead shift the LCM. In this way, there is a well-known relationship between the LCM shift and the equivalent offset frequency according to the linear spatial dispersion of the pulse shaper. The spectral resolution of our shaper is 2.6 GHz, ultimately limited by the spot size of the comb lines on the mask. This resolution limit has been measured by scanning a tunable narrow-linewidth cw laser with the LCM replaced by a narrow slit. Each spectral line is controlled by every two pixels of the LCM when the mode-locked laser is operated at 9 GHz, as mentioned above. This method for offset frequency emulation is valid if the mode-locked laser is stable or, alternatively, has offset frequency fluctuations varying around an average value, which will be confirmed by our experimental results given below. Figure 5 shows typical averaged scope traces (average of 50 times) for (a) 0%, (b) 25%, and (c) 50% offset, respectively. Note that in the latter case, we find a residual peak-pulse intensity at $T/2$ that we attribute to a slight ringing in the electrical response of our photodiode and measurement system. We have performed similar measurements for different offsets, by shifting the LCM, and the ratio $\Delta$ has been calculated from the averaged scope traces. In Fig. 4, we show pulse-contrast ratios superimposed with the theoretical curve. We find excellent agreement between the experimental data and the simulation results.

## 3. ESTIMATION OF COMB OFFSET FREQUENCY FLUCTUATIONS

The experimental results reported in Section 2 are the result of averaged time-domain waveform measurements and, therefore, may be understood largely in terms of static comb shifts. In this section, we consider nonaveraged sampling scope traces, aimed at analyzing time-varying changes in the comb offset frequency. Figure 6 shows typical scope traces (overlap of 100 scans) together with the corresponding averaged waveforms for a 9 GHz mode-locking rate and different optical comb offsets. For 0% offset, shown in Fig. 6(a), very clear sampling scope traces are generated. In contrast, for ~25% and ~50% offsets, Figs. 6(b) and 6(c), respectively, the resultant scope traces are noisy. Intensity noise is mainly found in the regions between the pulse positions in the absence of pulse shaping (at $T/2$ and odd multiples). Much weaker fluctuations, if any, are observed at the time locations of the input pulses. The dependence of time-domain noise on offset frequency is consistent with the change of the parameter $\Delta$ as a function of the offset frequency shown in Fig. 4.

In Fig. 7(a), we show a histogram that represents the distribution of relative offset frequency obtained by converting the measured intensity noise at $T/2$, in Fig. 6(b), into frequency noise via the calibration curve derived in Section 2, shown in Fig. 4. The data in Fig. 7(a) were obtained with the offset frequency biased at 25% offset. We have estimated the comb offset frequency fluctuations of the mode-locked laser to be ~237 MHz or 2.63% (calculated value of the standard deviation from this distribution). We performed additional experiments with larger phase-shifts for the two-valued periodic filter, i.e., $\Phi > \pi/2$. In all cases, comb shifts translate into variations in the modulation of the output multiplied train but, for specific offset intervals, the contrast is inverted ($\Delta > 1$). Similar to the case of $\Phi = \pi/2$, offset frequency fluctuations were estimated by intensity-noise to frequency-noise conversion. For example, when $\Phi = 5\pi/8$ and the offset

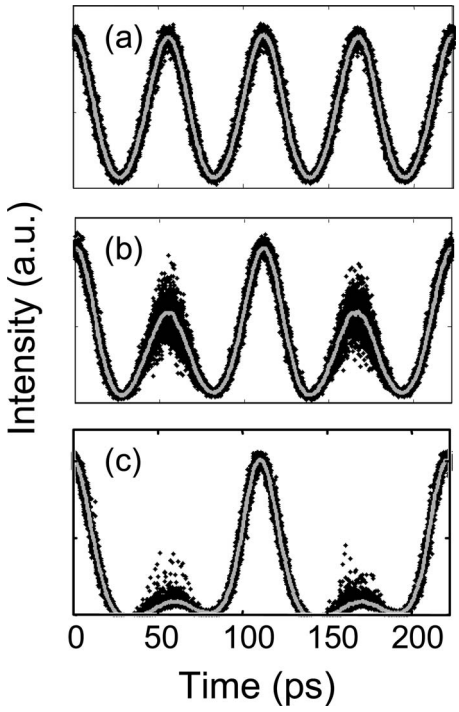


Fig. 6. Nonaveraged sampling scope traces for (a) 0%, (b) 25%, and (c) 50% offset frequency, respectively. The averaged traces are also shown.

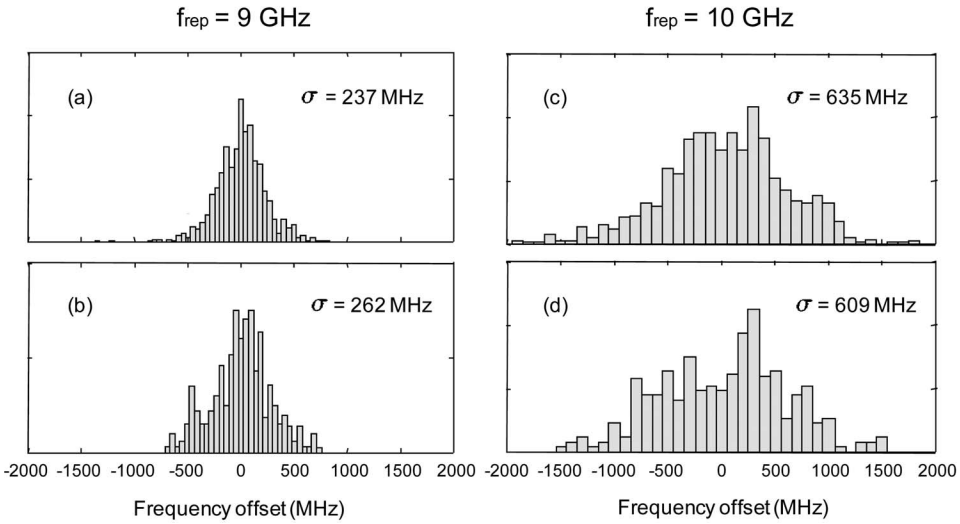


Fig. 7. Histograms representing the offset frequency distribution for the mode-locked laser running at (a) and (b) 9 GHz and (c) and (d) 10 GHz, respectively. Distribution (a) is obtained after time-domain intensity-noise to frequency-noise conversion, from Figs. 6(b) and 4. Histogram (b) is derived from the heterodyne beating between a cw laser and the comb [see Fig. 9(c)]. Histogram (c) is obtained by performing time-noise to frequency-noise conversion. Finally, offset frequency distribution (d) is obtained from the OSA traces in Fig. 11. Offset fluctuations are clearly more significant for the laser operating at 10 GHz.

frequency is biased at 25% offset, a value of ~243 MHz (2.70%) was obtained, which is close to the estimation made with $\Phi = \pi/2$.

We were unable to measure these comb shifts by using our OSA, as shown in Fig. 8, due to the limited spectral resolution (0.01 nm or 1.25 GHz). Therefore, to confirm the validity of our time-domain approach for estimating offset frequency fluctuations, we have determined the comb frequency instability by heterodyne beating with a 1 kHz linewidth cw laser. The combination of the cw laser with the comb generates, in the rf domain, a set of tones. Figures 9(a) and 9(b) show typical rf power spectra of one specific beat-signal, measured with an electrical spectrum analyzer (ESA). Figure 9(c) shows an overlap of 100 rf traces. By performing simple statistics, we obtain the frequency-noise distribution shown in Fig. 7(b), which yields a calculated beat-note-signal standard deviation of 262 MHz (2.91%), close to the prediction made with our line-by-line shaping approach. Inspection of Fig. 9(c) only provides the span of frequency-offset fluctuations, which coincides with the extension of the histogram in Fig. 7(b). The total number of traces in both the scope and ESA, Figs. 6(b) and 9(c), respectively, were the same (100), and the acquisition time per trace was around 3 s in each case. Therefore, the measurement bandwidth (observation time) for estimation of the frequency-offset fluctua-

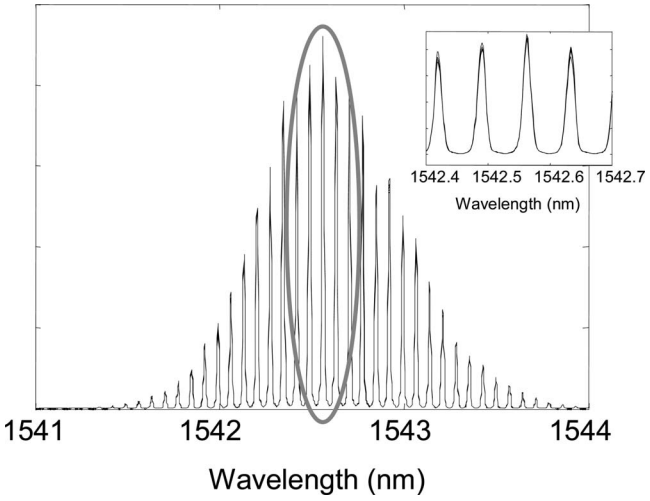


Fig. 8. Overlaid optical spectra (50 traces) of the mode-locked laser running at 9 GHz.

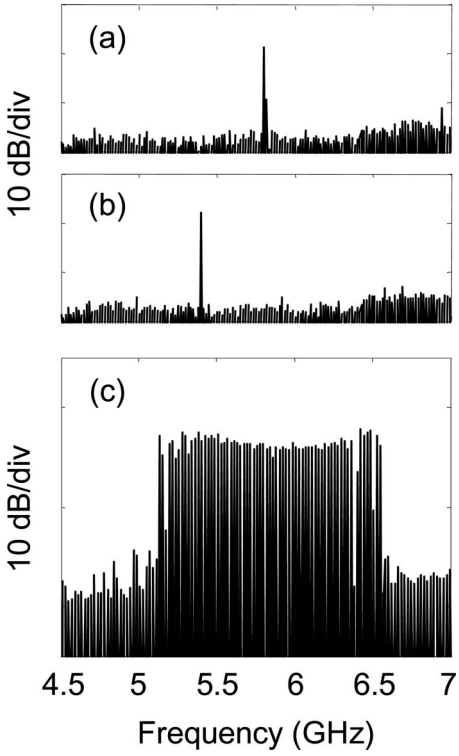


Fig. 9. Heterodyne beating between a cw laser and the frequency comb. (a) and (b) Typical rf power spectra of a beat note measured with an ESA. (c) Overlapped rf power spectra.

tions was similar, and thus the comparison of histograms in Fig. 7(a) and 7(b) is meaningful. On the other hand, due to the limited spectral resolution of the ESA when set for a wide (2.5 GHz) sweep, we could not determine from the heterodyne beat data of Fig. 9 whether the comb exhibits discrete fluctuations (jumps between supermodes spaced by the cavity resonance frequency, which is 8.3 MHz) or whether the offset frequency changes continuously (arbitrary fluctuations of the cavity length).

We have performed similar experiments with the harmonically mode-locked laser running at 10 GHz. A different spectral line-by-line shaper is employed to accurately match the spatial resolution with the new spectral line spacing. In earlier experiments [10] we found empirically that our laser exhibited larger offset frequency fluctuations when running at a 10 GHz repetition rate compared to a 9 GHz repetition rate. In experiments with simple spectral amplitude filters, we also observed quantitatively that these larger offset frequency fluctuations corresponded to substantially larger pulse shaping noise. Here we seek to quantify the pulse shaping noise and link it quantitatively to the degree of offset frequency variations. Figure 10 shows overlaid scope traces together with the corresponding averaged waveform for 25% offset frequency. Note that the sampling scope traces are clearly more noisy than the traces obtained when the laser is operating at 9 GHz [Fig. 6(b)]. The calculated offset frequency standard deviation is 635 MHz (6.35%), obtained by using the introduced intensity-noise to frequency-noise conversion approach. In Fig. 7(c), we show the corresponding histogram. In this regime of frequency noise, the offset fluctuations are directly observed with our OSA as shown in Fig. 11 (overlap of 50 scans). The acquisition time per trace was around 5 s, which leads to a total observation time comparable to that considered in the scope trace experiments. Note that comb fluctuations contribute to increase the effective linewidth of the spectral lines as highlighted in the inset of Fig. 11. Figure 7(d) shows the offset frequency distribution obtained from the OSA spectra in Fig. 11. The calculated comb fluctuation standard deviation from these OSA traces is 609 MHz (6.09%), which agrees very well with the prediction based on the line-by-line shaping approach.

## 4. CONCLUSIONS

We have analyzed the effect of frequency comb shifting on time-domain waveforms generated via free-space grating-based line-by-line pulse shaping. Specifically, a spectral phase-only line-by-line filter has been considered, which allowed us to evaluate, in a simple and intuitive way, the comb-offset variations from intensity-modulation changes in the resultant temporal waveform. As an application, we have estimated the offset fluctuations of a harmonically mode-locked fiber laser by examining the noise in the waveforms measured with a sampling scope. We found very good agreement between these estimations and frequency-noise measurements based on conventional approaches. Our results may be interesting for the development of novel comb stabilization techniques, e.g., detected waveform variations induced by comb fluctuations may be used as feedback signals in a loop configuration for the active control of the comb [14].

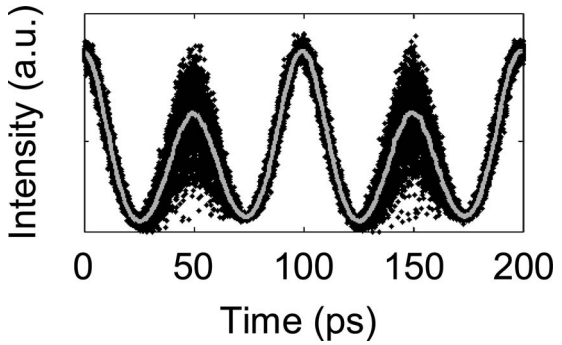


Fig. 10. Nonaveraged sampling scope traces for 25% offset frequency. The resultant averaged trace is also shown.

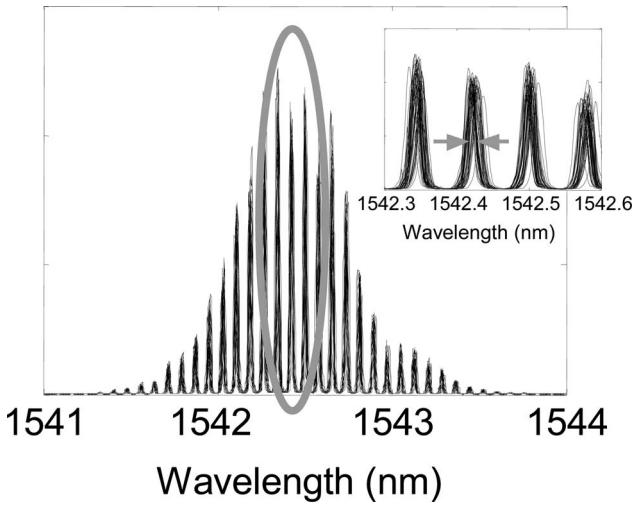


Fig. 11. Overlaid optical spectra of our mode-locked laser running at 10 GHz.

## ACKNOWLEDGMENTS

This work was supported in part by the Defense Advanced Research Projects Agency (DARPA)/Air Force Office of Scientific Research under grant FA9550-06-1-0189 and by the National Science Foundation (NSF) under grant ECCS-0601692. J. Caraquitena gratefully acknowledges the support of the Government of Spain through a Postdoctoral Fellowship from the Ministerio de Educación y Ciencia.

## REFERENCES

1. A. M. Weiner, "Femtosecond pulse shaping using spatial light modulators," Rev. Sci. Instrum. **71**, 1929–1960 (2000).
2. S. T. Cundiff, J. Ye, and J. L. Hall, "Optical frequency synthesis based on mode-locked lasers," Rev. Sci. Instrum. **72**, 3749–3771 (2001).
3. T. Udem, R. Holzwarth, and T. W. Hansch, "Optical frequency metrology," Nature **416**, 233–237 (2002).
4. L. S. Ma, Z. Y. Bi, A. Bartels, L. Robertsson, M. Zucco, R. S. Windeler, G. Wilpers, C. Oates, L. Hollberg, and S. A. Diddams, "Optical frequency synthesis and comparison with uncertainty at the $10^{-19}$ level," Science **303**, 1843–1845 (2004).
5. Z. Jiang, D. E. Leaird, and A. M. Weiner, "Line-by-line pulse shaping control for optical arbitrary waveform generation," Opt. Express **13**, 10431–10439 (2005).

6. Z. Jiang, C.-B. Huang, D. E. Leaird, and A. M. Weiner, "Optical arbitrary waveform processing of more than 100 spectral comb lines," Nat. Photonics **1**, 463–467 (2007).
7. N. K. Fontaine, R. P. Scott, J. Cao, A. Karalar, W. Jiang, K. Okamoto, J. P. Heritage, B. H. Kolner, and S. J. B. Yoo, "32 phase ×32 amplitude optical arbitrary waveform generation," Opt. Lett. **32**, 865–867 (2007).
8. K. Takiguchi, K. Okamoto, T. Kominato, H. Takahashi, and T. Shibata, "Flexible pulse waveform generation using silica-waveguide-based spectrum synthesis circuit," Electron. Lett. **40**, 537–538 (2004).
9. D. Miyamoto, K. Mandai, T. Kurokawa, S. Takeda, T. Shioda, and H. Tsuda, "Waveform-controllable optical pulse generation using an optical pulse synthesizer," IEEE Photon. Technol. Lett. **18**, 721–723 (2006).
10. Z. Jiang, D. S. Seo, D. E. Leaird, and A. M. Weiner, "Spectral line-by-line pulse shaping," Opt. Lett. **30**, 1557–1559 (2005).
11. C.-B. Huang, Z. Jiang, D. E. Leaird, and A. M. Weiner, "The impact of optical comb stability on waveforms generated via spectral line-by-line pulse shaping," Opt. Express **14**, 13164–13176 (2006).
12. J. Azaña and M. A. Muriel, "Temporal self-imaging effects: theory and application for multiplying pulse repetition rates," IEEE J. Sel. Top. Quantum Electron. **7**, 728–744 (2001).
13. J. Caraquitena, Z. Jiang, D. E. Leaird, and A. M. Weiner, "Tunable pulse repetition-rate multiplication using phase-only line-by-line pulse shaping," Opt. Lett. **32**, 716–718 (2007).
14. C. DeCusatis and L. Jacobowitz, "Wavelength locked loops for optical communication systems," in *Proceedings of IEEE Sarnoff Symposium, Session S13*, (Proc. IEEE 2007), pp. 48–52.